INVESTIGATION OF KERF TAPER ANGLE AND SURFACE ROUGHNESS IN ABRASIVE WATER JET MACHINED GLASS FIBER-REINFORCED POLYESTER COMPOSITES

UDC:678.674:621.7.044.4
Original scientific paper https://doi.org/10.46793/adeletters.2025.4.4.1

Karthick Rasu[1*], Joao Paulo Davim[2], Ramesh Marimuthu[3], Vigneshkumar Murugesan[4]

[1]Department of Mechanical Engineering, Velammal College of Engineering and Technology, Madurai 625 009, Tamil Nadu, India
[2]Department of Mechanical Engineering, University of Aveiro, Campus Santiago, 3810-193 Aveiro, Portugal
[3]Department of Mechanical Engineering, M.P. Nachimuthu M. Jaganathan Engineering College, Erode 638 112, Tamil Nadu, India
[4]Department of Mechanical Engineering, Sri Krishna College of Engineering and Technology, Coimbatore 641 008, Tamil Nadu, India

Abstract:
Glass fiber-reinforced polymer (GFRP) composites are commonly used in aerospace, automotive, and structural applications due to their excellent strength-to-weight ratio and resistance to corrosion. Conventional machining methods, however, still face persistent difficulties in maintaining dimensional accuracy and producing smooth surface finishes. Abrasive Water Jet Machining (AWJM) offers a non-traditional alternative with improved performance, though limited studies address its effects across varying material thicknesses. This study investigates the influence of AWJM parameters, water pressure (250–350 MPa), traverse speed (1500–2500 mm/min), and stand-off distance (2–4 mm) on kerf taper angle and surface roughness in 3 mm and 6 mm thick GFRP laminates. The composites were fabricated using hand lay-up and compression molding. Experiments were designed using an L9 Taguchi orthogonal array with signal-to-noise (S/N) ratio analysis under the "Smaller is Better" criterion. Results showed that stand-off distance contributed the most to kerf taper (54.26% for 3 mm) and surface roughness (80.25% for 3 mm), while water pressure dominated in thicker laminates (56.63% for 6 mm taper, 22.79% for roughness). The optimal combination of 350 MPa water pressure, 1500 mm/min traverse speed, and 2 mm stand-off distance achieved a minimum kerf taper of 1.05° and surface roughness of 2.0 µm in 3 mm laminates, compared to 1.20° and 2.3 µm in 6 mm laminates. These findings provide a quantitative basis for optimizing AWJM parameters to improve machining quality in GFRP components for lightweight engineering applications.

ARTICLE HISTORY
Received: 30 June 2025
Revised: 3 September 2025
Accepted: 25 September 2025
Published: 15 December 2025

KEYWORDS
Kerf taper angle, Surface roughness, Glass fiber, Polyester resin, Abrasive water jet machining

1. INTRODUCTION

GFRP composites are extensively used in aerospace, automotive, marine, and structural applications owing to their high strength-to-weight ratio, corrosion resistance, and ease of fabrication [1]. However, due to their anisotropic and heterogeneous nature, these materials exhibit complex behavior during machining operations. When fiber-reinforced composites are machined using conventional methods, problems such as heat build-up, fiber pull-out, delamination, and heavy tool wear are quite common. These issues usually affect both the accuracy of the cut and the finish of

*CONTACT: Karthick Rasu, e-mail: rkarthick33@gmail.com

the surface. As a result, AWJM has emerged as a practical alternative for cutting such materials [2,3]. Abrasive water jet machining offers several benefits, including the absence of thermal distortion, very little mechanical stress on the material, and the capability to cut complex shapes even in materials that are normally difficult to machine [4]. The cutting quality in abrasive water jet machining is strongly influenced by process parameters such as water pressure (WP), traverse speed (TS), and standoff distance (SOD). These factors directly affect the kerf taper angle (ϑ) and surface roughness (*Ra*), which are especially important in applications that demand high precision [5].

Thakur et al. [6] reported that the AWJM performance of woven GFRP laminates depends strongly on fiber density. The 610 GSM laminate exhibited lower delamination and surface damage than the 210 GSM laminate during AWJM, while also possessing superior mechanical strength. They further observed [6] that process parameters such as traverse speed and water pressure play a decisive role in controlling delamination extent (DE) and *Ra*, with optimized conditions, low traverse rate, and high water pressure (WP) enhancing machining quality. Field Emission Scanning Electron Microscope (FESEM) analysis confirmed these findings by revealing smoother machined surfaces and reduced fiber pull-out in the 610 GSM laminate.

Dahiya et al. [7] reported that AWJM is effective for machining GFRP composites. They studied the effects of water pressure, standoff distance, traverse rate, and abrasive flow on (surface roughness) *Ra*, *kerf taper,* and max. delamination, and used response surface methodology (RSM) and Taguchi methods for optimization. Results showed significant improvement in responses with the RSM-Desirability approach, further validated by Scanning Electron Microscope (SEM) analysis. Dahiya et al. [8] investigated AWJM of GFRP composites considering water pressure, stand-off distance, traverse rate, and abrasive flow rate. Using RSM-based modelling, they found that higher water pressure and abrasive flow, along with lower traverse rate and stand-off distance, reduced delamination, surface roughness, and kerf taper. Multi-response optimization achieved high desirability with errors below 8%, confirming model accuracy. Dahiya et al. [9] reported that AWJM is widely used for cutting and shaping hard-to-machine composites. In this study, glass fiber composites were machined using AWJM, considering water pressure, traverse speed, standoff distance, and abrasive mass flow rate. The experiments were designed with Taguchi's method in Minitab 18, and ANOVA was applied to evaluate the significance of process parameters on cutting performance.

Alrasheed [10] applied Artificial Neural Network (ANN), Genetic Algorithm (GA), Particle Swarm Optimization (PSO), Simulated Annealing (SA), and Least Squares Estimation (LSE) techniques to optimize AWJM parameters for Glass/Carbon Fiber Reinforced Composite (FRC) materials. Among these, LSE showed the best performance, achieving the lowest Root Mean Square Error (RMSE) for *Ra*, kerf width, and Material Removal Rate (MRR). SA and PSO also yielded competitive results, while ANN and GA were less effective. The study highlights LSE, SA, and PSO as efficient tools for AWJM parameter optimization.

Singh and Thakur [11] studied AWJM of Multi-Walled Carbon Nanotube (MECNT) reinforced GFRP composites, analyzing the effects of TS, WP, and standoff distance on kerf taper angle, surface roughness, MRR, and delamination. Using Taguchi and ANOVA methods, they identified key parameters influencing machining performance. The addition of Multi-Walled Carbon Nanotube (MWCNTs) improved kerf quality and surface finish, confirmed through surface morphology analysis.

Vikas and Srinivas [12] explored AWJM of E-glass/epoxy composites fabricated via hand lay-up and compression molding. They investigated the influence of TS, WP, Abrasive Flow Rate (AFR), SOD, and garnet size on kerf characteristics. The study identified garnet size, pressure, and standoff distance as key factors affecting kerf formation. SEM examination showed that while no delamination or abrasive particles were embedded, fiber pull-out occurred when the pressure was increased.

Manoj et al. [13] investigated the AWJM of glass fiber-reinforced laminates of different thicknesses, examining how pressure, standoff distance, and traverse rate influence the process. The study evaluated key responses, including top and bottom kerf widths as well as kerf taper, through ANOVA. SEM observations indicated very limited delamination, confirming that AWJM is well-suited for precision machining of polymer composites.

Jesthi et al. [14] examined the machinability and mechanical performance of plain glass, carbon, and hybrid ([CG2CG]S) fiber-reinforced composites, considering both dry conditions and those aged in seawater. Abrasive jet machining was used to evaluate MRR, *Ra*, and depth of cut (DOC). The study found improved flexural strength in hybrid

composites, with MRR and DOC increasing at higher pressures, particularly in seawater-aged samples.

Deepak and Ashwin Pai [15] examined the influence of abrasive water jet drilling parameters on hole diameter in GFRP composites reinforced with 2%, 4%, and 6% graphite. Using a Taguchi L9 design and a five-axis CNC AWJ setup, the effects of pressure, feed rate, and standoff distance were analyzed. Results indicated that jet pressure significantly impacts hole size, and graphite addition enhances the machinability of GFRP composites.

Prasad and Chaitanya [16] optimized AWJM parameters for drilling holes in GFRP composites using the Taguchi L9 orthogonal array. The study investigated the effects of AFR, WP, SOD, and fiber orientation on MRR, *Ra*, and hole quality. Results showed that standoff distance, pressure, and abrasive flow rate significantly influence MRR and hole accuracy. Optimal settings for high MRR and precise hole formation were identified, and analysis of means was used for statistical evaluation.

Muralidharan et al. [17] investigated the effect of abrasive flow rate, standoff distance, and traverse rate on taper angle and circularity during AWJM of E-glass/polypropylene composites. Using a Taguchi L16 design and ANOVA with Grey Relational Analysis, they found that standoff distance significantly influenced taper angle, while AFR had a major impact on circularity.

Ming et al. [18] addressed surface quality issues in trimming hybrid fiber-reinforced composites using AWJM. The effects of AFR, WP, SOD, and TS on surface roughness were studied. Using response surface methodology, they developed and validated a quadratic model, identifying AFR and SOD as the most influential parameters for minimizing *Ra*.

Thayananthan et al. [19] examined the influence of AWJM factors on the *Ra* of glass fiber reinforced (GFR) epoxy composites by Taguchi's technique and multiple linear regression analysis. ANOVA results revealed that abrasive type, WP, SOD, and AFR significantly influenced *Ra*, with AFR being the most dominant factor. The developed model effectively predicted Ra values within the experimental limits.

Armağan and Arici [20] analyzed AWJM performance on GFR vinyl ester composites using Taguchi design. Parameters such as SOD, AFR, TS, WP, and thickness were studied for their effects on top kerf width and surface roughness. ANOVA and regression analysis identified standoff distance as the most influential factor, with validated predictive models confirming optimal parameter settings.

Doreswamy et al. [21] studied the influence of AWJM parameters on kerf width in graphite-filled glass fiber epoxy composites using Taguchi L27 design. ANOVA revealed that feed rate, WP, and SOD significantly affect kerf width, contributing 52.16%, 24.72%, and 12.38% respectively. Regression models were developed, and SEM analysis confirmed minimal delamination at optimized settings.

Lemma et al. [22] conducted a comparative study on conventional and oscillating AWJ cutting of GFR composites. The oscillating technique, involving back-and-forth head motion, significantly improved surface finish. Stylus-based measurements showed up to 20% reduction in surface roughness (*Ra*) compared to normal AWJ cutting, demonstrating enhanced cut quality.

Recent research has given considerable attention to abrasive water jet machining (AWJM) of fiber-reinforced composites, highlighting its ability to deliver high-quality machining without causing thermal damage. Many studies have examined how process variables such as water pressure, traverse speed, and stand-off distance affect outcomes like *Ra*, kerf characteristics, and delamination. Nevertheless, much of the available work has been concentrated on thermoset-based laminates and within narrow AWJM parameter ranges, creating a gap in the detailed study of kerf taper angle and surface roughness in glass fiber-reinforced polyester composites of different thicknesses.

Thus, there remains a notable research gap in systematically correlating thickness-dependent variations with multi-response optimization of kerf taper and surface roughness using a unified composite system. This study addresses this gap by experimentally analyzing the simultaneous effects of key AWJM parameters on both kerf quality and surface roughness for 3 mm and 6 mm GFRP laminates, using Taguchi design, S/N ratio analysis, and contour mapping, thereby offering practical insights for high-precision composite machining in lightweight engineering applications.

2. MATERIALS AND METHODS

2.1. Materials

Glass fiber-reinforced polymer composites were prepared using a polyester resin system with E-glass fibers as reinforcement. The E-glass fibers were obtained from United Trading Corporation, Madurai, Tamil Nadu, India, to maintain uniform

quality during fabrication. Supplied in woven mat form, these fibers were chosen for their favorable strength-to-weight ratio, corrosion resistance, and compatibility with thermosetting resins [23].

The matrix material consisted of polyester resin, chosen for its ease of processing, good mechanical properties, and widespread use in composite applications. The resin was mixed with a methyl ethyl ketone peroxide hardener at the recommended ratio to initiate curing. All resin components were purchased from a local chemical supplier to ensure freshness and optimal reactivity.

2.2. Fabrication of Glass Fiber Composite

The GFR polyester composites were produced using a traditional hand lay-up technique followed by compression molding, with two thicknesses prepared 3 mm and 6 mm. Woven E-glass fiber mats served as the reinforcement, while unsaturated polyester resin was used as the matrix material. The resin mixture was formulated by blending the polyester resin with 1 wt.% methyl ethyl ketone peroxide as a curing agent and 0.5 wt.% cobalt naphthenate as an accelerator. Before starting the lay-up process, the surface of the metal mold was coated with a wax-based release agent to avoid adhesion. The glass fiber mats were cut to the required dimensions and placed in the mold. A prepared resin mixture was then applied uniformly over each layer, followed by rolling to achieve complete wetting and to eliminate entrapped air. The laminate assembly was subjected to a pressure of 1.5 MPa in a hydraulic press and allowed to cure under ambient conditions for 24 hours. Post-curing was subsequently carried out at 60°C for 2 hours to enhance the mechanical properties of the composite. Fig. 1 shows the raw glass fiber, the 3 mm thick specimen, and the 6 mm thick specimen.

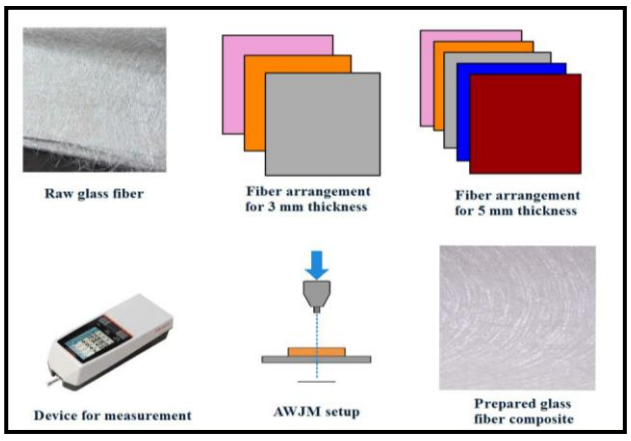

Fig. 1. Process of AWJM of composites

2.3. Experimental Work

The machining trials were carried out using a CNC-controlled AWJM system equipped with a high-pressure pump capable of delivering up to 350 MPa. The nozzle used had an orifice diameter of 0.76 mm and employed garnet abrasive particles (80 mesh size) with a constant AFR of 300 g/min. Flat composite laminates of glass fiber-reinforced polyester were prepared with two thicknesses (3 mm and 6 mm) and clamped firmly on the cutting bed to avoid vibration during machining.

The input process parameters selected for the experiments were WP (250, 300, and 350 MPa), TS (1500, 2000, and 2500 mm/min), and SOD (2, 3, and 4 mm). An L9 Taguchi orthogonal array was employed to systematically vary the parameters and evaluate their effects on kerf taper angle and surface roughness. Eq. 1 was used to find the kerf taper angle *(ϑ)*. After machining, the top and bottom kerf widths were measured using a digital profile projector with ±0.01 mm accuracy, and the kerf taper angle was computed using geometric relations. All tests were conducted under dry conditions at ambient temperature to ensure consistency. Table 1 presents the factors and their levels for AWJM of composites.

$$\vartheta = \tan^{-1}\left(\frac{Tw-Bw}{2t}\right) \quad (1)$$

Where are:
Tw – is the Top kerf width (mm),
Bw – is the Bottom kerf width (mm), and
t – is the Thickness of the material (mm).

Table 1. Factors and their levels for AWJM

Parameters	Abb.	Level 1	Level 2	Level 3
Water Pressure (MPa)	WP	250	300	350
Traverse Speed (mm/min)	TS	1500	2000	2500
Stand-off Distance (mm)	SOD	2	3	4

3. RESULTS AND DISCUSSION

The kerf taper angle *(ϑ)* and surface roughness (*Ra*) for the 3 mm and 6 mm thick composite specimens are presented in Tables 2 and 3, respectively.

Table 2. Kerf taper angle *(ϑ)* and surface roughness (*Ra*) for 3 mm thickness specimen

WP	TS	SOD	Kerf taper angle (°)	S/N ratio	Surface roughness (µm)	S/N ratio
250	1500	2	1.2	-1.58362	2.25	-7.04365
250	2000	3	1.36	-2.67078	2.95	-9.39644
250	2500	4	1.52	-3.63687	3.65	-11.2459
300	1500	3	1.15	-1.21396	2.6	-8.29947
300	2000	4	1.3	-2.27887	3	-9.54243
300	2500	2	1.1	-0.82785	2.2	-6.84845
350	1500	4	1.25	-1.9382	2.8	-8.94316
350	2000	2	1.05	-0.42379	2	-6.0206
350	2500	3	1.18	-1.43764	2.7	-8.62728

Table 3. Kerf taper angle *(ϑ)* and surface roughness (*Ra*) for 6 mm thickness specimen

WP	TS	SOD	Kerf taper angle (°)	S/N ratio	Surface roughness (µm)	S/N ratio
250	1500	2	1.4	-2.92256	2.6	-8.29947
250	2000	3	1.55	-3.80663	3.35	-10.5009
250	2500	4	1.7	-4.60898	4.1	-12.2557
300	1500	3	1.3	-2.27887	2.9	-9.24796
300	2000	4	1.45	-3.22736	3.4	-10.6296
300	2500	2	1.25	-1.9382	2.5	-7.9588
350	1500	4	1.38	-2.79758	3.05	-9.686
350	2000	2	1.2	-1.58362	2.3	-7.23456
350	2500	3	1.32	-2.41148	2.85	-9.0969

3.1. Analysis of Kerf Taper Angle

Kerf taper angle is a critical quality indicator in AWJM, especially when machining composite materials for lightweight engineering applications such as automotive and aerospace components. A lower kerf taper angle is desirable for improved dimensional accuracy, and thus the "Smaller is Better" S/N ratio criterion is applied.

The analysis of the kerf taper angle during AWJM of glass fiber-reinforced polyester composites revealed that the influence of process parameters varied significantly with specimen thickness. Based on the S/N ratios under the "Smaller is Better" criterion, the results for the 3 mm thick specimen (Table 4) showed that stand-off distance exhibited the highest influence on kerf taper angle (delta = 1.6729), followed by water pressure (delta = 1.3639), and traverse speed (delta = 0.3889). This is because, in thinner laminates, SOD plays a dominant role; as SOD increases, the jet diverges and loses kinetic energy before striking the surface, leading to a wider entry kerf and larger taper, whereas at lower SOD the jet remains concentrated, transferring maximum energy to the cut zone and producing straighter kerfs [24]. In contrast, for the 6 mm thick specimen (Table 5), water pressure emerged as the most significant factor (delta = 1.515), followed by stand-off distance (delta = 1.397), while traverse speed remained the least influential (delta = 0.320). This variation can be explained by the role of WP in cutting thicker laminates. At higher WP, the jet attains greater energy, which accelerates abrasive particles and improves material removal efficiency. This reduces the kerf taper by enabling the jet to cut through the full thickness of the specimen. In contrast, at lower WP, the jet energy becomes inadequate, causing incomplete cutting and a larger difference between the top and bottom kerf widths. TS, though the least significant factor, also influences taper by regulating the jet–material interaction time. A higher TS decreases the energy delivered per unit length, resulting in incomplete cutting and higher taper, while a lower TS increases the energy transfer, thereby improving the straightness of the cut [25].

These findings show that in thin laminates, kerf taper is mainly influenced by jet focus and energy dissipation, which are governed by the SOD. In thicker laminates, however, sufficient WP is required to overcome resistance to jet penetration. Thus, accurate control of WP and SOD is vital for minimizing kerf taper in AWJM of composite laminates, ensuring better dimensional accuracy and enhancing their suitability for lightweight engineering structures.

Table 4. Response table for SN ratios for 3 mm specimen

Parameters	Level			Delta	Rank
	1	2	3		
WP	-2.6304	-1.4402	-1.2665	1.3639	2
TS	-1.5786	-1.7911	-1.9675	0.3889	3
SOD	-0.9451	-1.7741	-2.618	1.6729	1

Table 5. Response table for SN ratios for 6 mm specimen

Parameters	Level			Delta	Rank
	1	2	3		
WP	-3.779	-2.481	-2.264	1.515	1
TS	-2.666	-2.873	-2.986	0.32	3
SOD	-2.148	-2.832	-3.545	1.397	2

The ANOVA results for S/N ratios of 3 mm and 6 mm specimens are summarized in Tables 6 and 7, respectively. For the 3 mm specimen (Table 6), stand-off distance contributed the most (54.26%)

towards surface roughness variation, followed by water pressure (42.74%), while traverse speed showed only a minor effect (2.94%). This indicates that, in thinner laminates, surface finish is highly dependent on the degree of jet dispersion caused by stand-off distance, while adequate water pressure is still necessary to maintain jet energy for material removal. For the 6 mm specimen (Table 7), water pressure was the dominant factor with a contribution of 56.63%, followed by stand-off distance (41.14%), with traverse speed again showing negligible influence (2.22%). This shift demonstrates that in thicker specimens, jet energy (governed by water pressure) plays a more critical role in achieving smooth surfaces, whereas in thinner specimens, the focus of the jet (stand-off distance) is more decisive. In both cases, residual error was very low, confirming the validity of the model and reliability of the experimental results.

Table 6. ANOVA for SN ratios for 3 mm specimen

Source	DF	Seq SS	Adj SS	Adj MS	F	P	% of Contribution
WP	2	3.30692	3.30692	1.65346	651.93	0.002	42.74
TS	2	0.22748	0.22748	0.11374	44.84	0.022	2.94
SOD	2	4.19796	4.19796	2.09898	827.59	0.001	54.26
Error	2	0.00507	0.00507	0.00254	-	-	0.07
Total	8	7.73742	-	-	-	-	100.00

Table 7. ANOVA for SN ratios for 6 mm specimen

Source	DF	Seq SS	Adj SS	Adj MS	F	P	% of Contribution
WP	2	4.02750	4.02750	2.01375	2688.81	0.000	56.63
TS	2	0.15777	0.15777	0.07888	105.33	0.009	2.22
SOD	2	2.92576	2.92576	1.46288	1953.28	0.001	41.14
Error	2	0.00150	0.00150	0.00075	-	-	0.02
Total	8	7.11253	-	-	-	-	100.00

Fig. 2 illustrates the main effects plot for the mean signal-to-noise (S/N) ratios corresponding to the kerf taper angle of the 3 mm thick glass fiber-reinforced polyester composite specimens, machined using AWJM.

The S/N ratios were calculated based on the "Smaller is Better" criterion, aiming to minimize kerf taper for improved dimensional accuracy. Among the three parameters studied (WP, TS and SOD) the stand-off distance demonstrates the most momentous impact on kerf taper angle, as evidenced by the steep slope in its plot line. As the stand-off distance rises from 2 mm to 4 mm, the S/N ratio decreases substantially, indicating a worsening kerf taper. This behavior is consistent with the literature, where increased nozzle distance leads to loss of jet focus and greater energy dispersion, thereby increasing the taper [26].

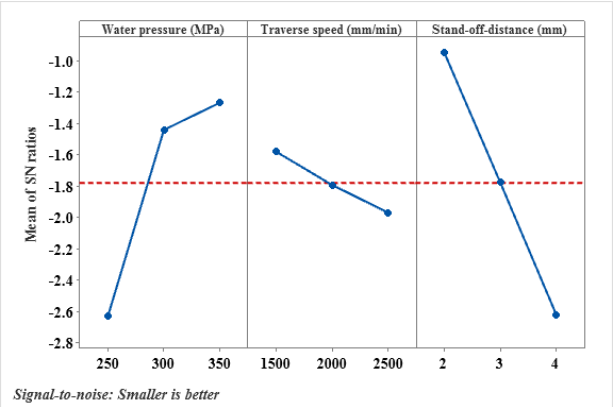

Fig. 2. Mean of SN ratio for 3 mm specimen

Water pressure exerts a significant effect, with an increase from 250 MPa to 350 MPa leading to higher S/N ratios and thereby indicating reduced kerf taper. This observation is consistent with earlier reports, as higher water pressure improves jet kinetic energy and cutting efficiency, which minimizes taper formation, particularly in thin composite laminates [27]. In contrast, traverse speed shows a comparatively moderate influence, with the S/N ratio gradually decreasing as speed rises from 1500 mm/min to 2500 mm/min. This suggests that although higher speeds reduce the interaction time between the jet and the material,

their effect on taper is relatively less pronounced than that of other parameters, in agreement with the findings of [28].

Overall, the best combination of factors for minimizing kerf taper in 3 mm specimens can be identified from the highest S/N levels as: Water pressure at 350 MPa, TS at 1500 mm/min, and SOD at 2 mm. These results highlight the significance of precise process control in AWJM to achieve high-dimensional accuracy, particularly in lightweight engineering components.

Fig. 3 illustrates the main effects plot based on the S/N ratios related to the θ in 6 mm thick glass fiber-reinforced polyester composites, machined using AWJM. The analysis is based on the "Smaller is Better" criterion, intending to minimize the kerf taper. Among the three process parameters, water pressure shows the most significant influence.

The S/N ratio improves considerably as the water pressure increases from 250 MPa to 350 MPa, indicating a substantial reduction in kerf taper at higher pressures. The stand-off distance also has a strong impact, as observed from the steep drop in the S/N ratio with increasing distance from 2 mm to 4 mm. This suggests that greater nozzle distance leads to increased kerf taper due to reduced jet focus. On the other hand, traverse speed exhibits a relatively mild effect, with a gradual decline in the S/N ratio as the speed increases from 1500 mm/min to 2500 mm/min.

Based on the S/N ratio trends in Fig. 2, the optimal parameters for minimizing kerf taper in 6 mm specimens are: WP at 350 MPa, TS at 1500 mm/min, and SOD at 2 mm. These results highlight the importance of controlling water pressure and stand-off distance, particularly when machining thicker composite laminates.

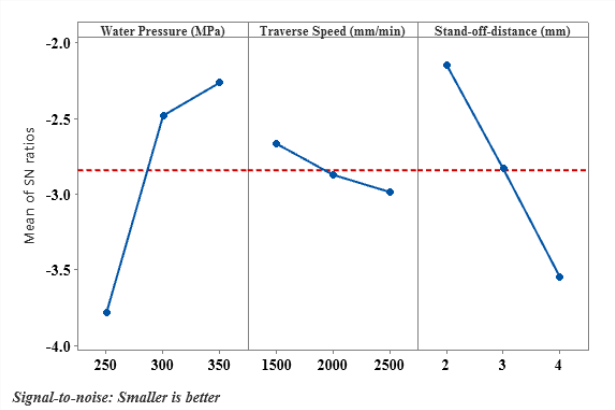

Fig. 3. Mean of SN ratio for 6 mm specimen

Fig. 4 presents contour plots illustrating the variation in kerf taper angle with respect to WP, TS, and SOD for two different material thicknesses (3 mm and 6 mm) in AWJM.

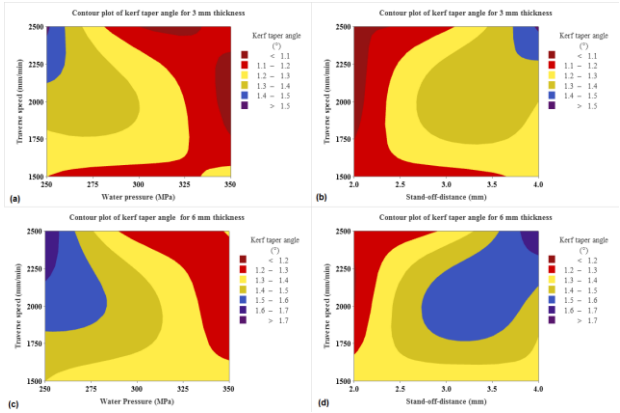

Fig. 4. Contour plot of kerf taper angle, (a) Water pressure vs Traverse speed for 3 mm thick, (b) Standoff distance vs Traverse speed for 3 mm thick, (c) Water pressure vs Traverse speed for 6 mm thick, (d) Standoff distance vs Traverse speed for 6 mm thick

For the 3 mm specimen (Figs. 4a and 4b), lower kerf taper angles (<1.1°) were observed at high water pressure (above 325 MPa), low traverse speed (below 1750 mm/min), and low stand-off distance (around 2.0 mm). As TS and SOD increased, the kerf taper angle increased significantly, reaching values greater than 1.5°, indicating less favorable cutting conditions. In contrast, the 6 mm thick specimen (Figs. 4c and 4d) exhibited generally higher kerf taper angles across all parameter settings. The lowest taper angles (1.3°–1.4°) were observed at moderate water pressures (275–300 MPa), traverse speeds around 1750–2000 mm/min, and stand-off distances of 3.0–3.5 mm. However, higher water pressures and increased traverse speeds or stand-off distances led to kerf taper values exceeding 1.7°. These trends indicate that material thickness significantly influences kerf quality, with thinner specimens showing better taper control, and that optimal combinations of process parameters are critical to minimizing taper in precision cutting applications [29].

3.2. Analysis of Surface Roughness

S/N ratio analysis for surface roughness was conducted using the "Smaller is Better" criterion to identify the most effective AWJM parameters for achieving smoother surfaces in glass fiber-reinforced polyester composites. The results are presented in Table 8 (3 mm specimens) and Table 9 (6 mm specimens). For the 3 mm thick specimen, SOD emerged as the most influential factor (delta =

3.273), followed by water pressure (delta = 1.365), and traverse speed (delta = 0.812). The mechanism behind this trend is that, at higher SOD, the jet loses focus and spreads before striking the material, which reduces cutting efficiency and leaves an irregular surface with higher roughness [30]. Conversely, at lower SOD (2 mm), the abrasive jet remains concentrated, producing finer cutting action and less fiber pull-out, which leads to smoother surfaces. This is further supported by the optimal parameter set of 2 mm SOD, 350 MPa WP, and 1500 mm/min TS, where the highest mean S/N ratio values were observed. For the 6 mm thick specimen, a similar trend was noted, with SOD again being the most dominant factor (delta = 3.026), followed by water pressure (delta = 1.680), and traverse speed (delta = 0.693). In thicker laminates, low SOD ensures that jet energy is delivered effectively throughout the depth, minimizing secondary erosion effects that can roughen the cut. Meanwhile, higher WP improves the material removal rate by accelerating abrasive particles, which helps in reducing micro-chipping and fiber–matrix debonding, thereby improving surface finish. Traverse speed, although the least influential parameter, still affects the jet–material interaction time. Lower speeds promote smoother surfaces by enabling consistent energy transfer, whereas higher speeds reduce contact time and lead to increased surface irregularities [31]. Overall, the results demonstrate that SOD is the most influential factor in controlling surface roughness in both thin and thick specimens. WP provides a secondary contribution by improving jet penetration and stability, whereas traverse speed (TS) exerts the least influence due to its limited role in energy delivery. Thus, precise regulation of SOD and WP is essential for obtaining high surface quality in AWJM of composite laminates, which is crucial for applications that demand dimensional accuracy and superior surface finish.

Table 8. Response table for SN ratios for 3 mm specimen

Parameters	Level			Delta	Rank
	1	2	3		
WP	-9.229	-8.23	-7.864	1.365	2
TS	-8.095	-8.32	-8.907	0.812	3
SOD	-6.638	-8.774	-9.91	3.273	1

Table 9. Response table for SN ratios for 6 mm specimen

Parameters	Level			Delta	Rank
	1	2	3		
WP	-10.352	-9.279	-8.672	1.68	2
TS	-9.078	-9.455	-9.77	0.693	3
SOD	-7.831	-9.615	-10.857	3.026	1

The ANOVA results for S/N ratios of the 3 mm and 6 mm specimens are presented in Tables 10 and 11, respectively. For the 3 mm specimen (Table 10), stand-off distance was identified as the most significant factor, contributing 80.25% to the variation, followed by water pressure at 14.50%, while traverse speed showed only a minor effect of 5.11%. The dominance of stand-off distance at smaller thickness indicates that jet dispersion and focus have a strong influence on surface characteristics, as even slight variations in jet distance affect the cutting precision and energy concentration on thinner laminates. In contrast, the ANOVA for the 6 mm specimen (Table 11) revealed that stand-off distance again played the leading role with 72.91% contribution, while water pressure contributed 22.79%, and traverse speed remained relatively insignificant at 3.79%. This shows that for thicker sections, although stand-off distance continues to be critical, the influence of water pressure increases because higher jet energy is required to penetrate and maintain cutting efficiency across the depth. The residual errors for both cases were minimal, confirming the adequacy and reliability of the model.

Table 10. ANOVA for SN ratios for 3 mm specimen

Source	DF	Seq SS	Adj SS	Adj MS	F	P	% of Contribution
WP	2	2.9945	2.9945	1.49725	100.66	0.010	14.50
TS	2	1.0543	1.0543	0.52717	35.44	0.027	5.11
SOD	2	16.5687	16.5687	8.28434	556.97	0.002	80.25
Error	2	0.0297	0.0297	0.01487	-	-	0.14
Total	8	20.6472	-	-	-	-	100.00

Table 11. ANOVA for SN ratios for 6 mm specimen

Source	DF	Seq SS	Adj SS	Adj MS	F	P	% of Contribution
WP	2	4.3402	4.3402	2.17012	44.76	0.022	22.79
TS	2	0.7216	0.7216	0.36078	7.44	0.118	3.79
SOD	2	13.8835	13.8835	6.94173	143.18	0.007	72.91
Error	2	0.0970	0.0970	0.04848	-	-	0.51
Total	8	19.0422	-	-	-	-	100.00

Fig. 5 illustrates the main effects plot for the mean S/N ratios of the 3 mm thick specimen, considering the "smaller is better" standard to minimize surface roughness.

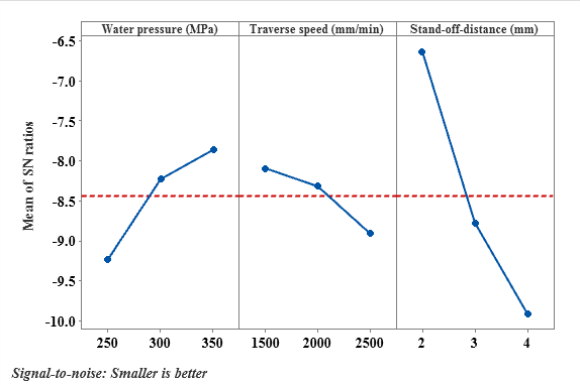

Fig. 5. Mean of SN ratio for 3 mm specimen

The results reveal that water pressure significantly influences surface quality, with an increasing trend in S/N ratio from 250 MPa to 350 MPa, indicating improved surface finish at higher pressures. Similarly, the traverse speed shows a slight improvement in surface quality at 1500 mm/min compared to higher speeds, suggesting that lower speeds favor reduced roughness. In contrast, the stand-off distance exhibits a strong negative effect; increasing the distance from 2 mm to 4 mm results in a substantial deterioration of the S/N ratio. Among the parameters studied, the stand-off distance has the most pronounced impact [32]. The optimal parameter settings for achieving minimal surface roughness in the 3 mm specimen are identified as 350 MPa WP, 1500 mm/min TS, and 2 mm SOD.

Fig. 6 shows the main effects plot for the mean S/N ratios of the 6 mm thick specimen, evaluated using the "smaller is better" standard for minimizing surface roughness.

The plot indicates that surface quality improves with increasing water pressure, with the S/N ratio increasing from 250 MPa to 350 MPa. This suggests that higher water pressure leads to smoother surfaces. For traverse speed, the best result is obtained at 1500 mm/min, while increasing the speed to 2500 mm/min results in a slight deterioration in surface finish. A significant influence is observed in the case of SOD, where increasing the distance from 2 mm to 4 mm leads to a steep decline in the S/N ratio, indicating poorer surface quality. Among all parameters, the stand-off distance has the most substantial effect [33]. The optimal combination for minimizing surface roughness in the 6 mm specimen is 350 MPa WP, 1500 mm/min TS, and 2 mm SOD.

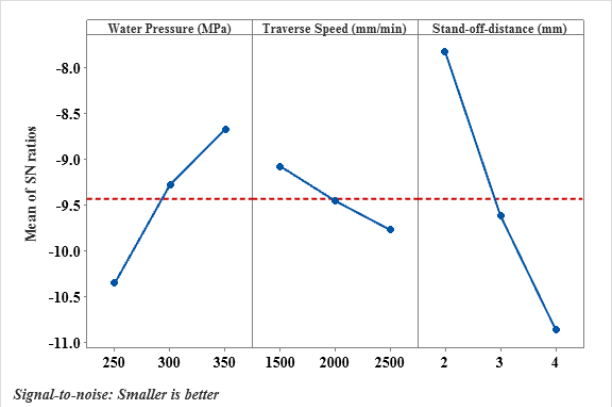

Fig. 6. Mean of SN ratio for 6 mm specimen

Fig. 7 shows contour plots representing the effect of process parameters on the surface roughness for 3 mm and 6 mm thick specimens machined using AWJM.

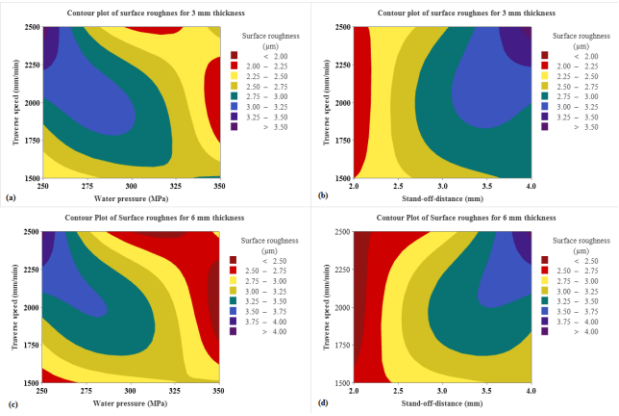

Fig. 7. Contour plot of surface roughness, (a) Water pressure vs Traverse speed for 3 mm thick, (b) Standoff distance vs Traverse speed for 3 mm thick, (c) Water pressure vs Traverse speed for 6 mm thick, (d) Standoff distance vs Traverse speed for 6 mm thick

For the 3 mm specimen (Figs. 7a and 7b), lower surface roughness values (<2.25 µm) were achieved at moderate water pressures (275–300 MPa), low TS (1500–1750 mm/min), and lower SOD (2.0–2.5 mm). As the TS and SOD increased, surface roughness also increased, with values exceeding 3.5 µm observed in the high stand-off and high-speed regions. For the 6 mm specimen (Figs 7c and 7d), the overall surface roughness values were comparatively higher. Surface roughness values below 2.75 µm were achieved at lower traverse speeds and moderate water pressures (275–300 MPa). However, higher traverse speeds and stand-off distances resulted in rougher surfaces, with roughness exceeding 4.0 µm. These observations indicate that surface finish deteriorates with increasing thickness, TS, and SOD, while optimal surface quality can be achieved by maintaining moderate WP and minimizing both TS and SOD.

4. CONCLUSION

This study investigated how abrasive water jet machining (AWJM) parameters affect kerf taper angle and surface roughness in glass fiber-reinforced polyester (GFRP) composites of two thicknesses (3 mm and 6 mm). Experimental results, supported by signal-to-noise (S/N) ratio analysis and contour plots, showed that stand-off distance had the strongest influence on both kerf taper and surface roughness, followed by water pressure, while traverse speed had a relatively lesser effect. For the 3 mm thick specimens, the lowest kerf taper angles (<1.1°) and finest surface roughness values (<2.25 µm) were obtained at a stand-off distance of 2 mm, water pressure of 350 MPa, and traverse speed of 1500 mm/min. A comparable trend was noted for the 6 mm thick specimens, although both kerf taper and surface roughness were generally higher due to the increased thickness, which reduced jet penetration efficiency and energy concentration. These results emphasize the importance of precise control of AWJM parameters, particularly stand-off distance and water pressure, to improve dimensional accuracy and surface integrity in composite machining. The study further demonstrates that, regardless of material thickness, maintaining a low stand-off distance and high-water pressure is essential for minimizing kerf taper and producing smoother surfaces.

Despite these promising results, certain limitations should be noted. The study examined only three machining parameters at selected levels, while other influential factors such as abrasive grain size, nozzle wear, fiber orientation, and multi-pass cutting were not considered. Furthermore, the analysis was limited to surface quality responses, without addressing mechanical properties such as residual strength, fatigue behavior, and delamination under service conditions.

Future research should extend the scope of process variables, examine a broader range of composite systems, and include additional response factors such as mechanical performance. The use of advanced predictive models or hybrid optimization strategies could also provide further improvements in machining accuracy and efficiency.

The findings offer practical guidelines for selecting machining parameters that ensure high surface quality and dimensional accuracy in GFRP components. Industries such as aerospace, automotive, and structural engineering, where stringent tolerances and high-quality surfaces are essential, can particularly benefit from the optimized parameter ranges identified in this work.

CONFLICTS OF INTEREST

The author declares no conflict of interest.

REFERENCES

[1] K. Rasu, A. Veerabathiran, Effect of red mud on mechanical and thermal properties of agave sisalana/glass fiber–reinforced hybrid composites. *Materials Testing*, 65(12), 2023: 1879–1889. https://doi.org/10.1515/mt-2023-0118.

[2] R.K. Thakur, K.K. Singh, Evaluation of advanced machining processes performance on filler-loaded polymeric composites: a state-of-the-art review. *Journal of the Brazilian Society of Mechanical Sciences and Engineering*, 43(6), 2021: 300. https://doi.org/10.1007/s40430-021-03027-z

[3] A.K. Dahiya, B.K. Bhuyan, S. Kumar, Perspective study of abrasive water jet machining of composites — a review. *Journal of Mechanical Science and Technology*, 36(1), 2022: 213–224. https://doi.org/10.1007/s12206-021-1220-x

[4] R.K. Thakur, K.K. Singh, Abrasive waterjet machining of fiber-reinforced composites: a state-of-the-art review. *Journal of the Brazilian Society of Mechanical Sciences and Engineering*, 42(7), 2020: 381. https://doi.org/10.1007/s40430-020-02463-7

[5] K. Rasu, A. Veerabathiran, V. Murugesan, G. Gopal, S.B. Muthusamy, G.A. Prabhu, Effect of process parameters on abrasive water jet

machining of natural and synthetic fibre reinforced polymer composites: a review. *International Journal of Abrasive Technology (IJAT),* 12(4), 2024: 10067601. https://doi.org/10.1504/IJAT.2024.10067601

[6] R.K. Thakur, K.K. Singh, M.T.A. Ansari, Influence of fabric areal density in woven GFRP laminate on abrasive water jet drilling responses. *Materials and Manufacturing Processes*, 38(9), 2023: 1119–1129. https://doi.org/10.1080/10426914.2022.2146719

[7] A.K. Dahiya, B.K. Bhuyan, V. Acharya, A.K. Kaushik, S. Kumar, Simultaneous optimization of process parameters during abrasive water jet machining on glass fibre reinforced polymer. *International Journal on Interactive Design and Manufacturing (IJIDeM),* 18(7), 2024: 5077–5094. https://doi.org/10.1007/s12008-023-01539-7

[8] A.K. Dahiya, B.K. Bhuyan, S. Kumar, Abrasive water jet machining of glass fibre reinforced polymer composite: experimental investigation, modelling and optimization. *International Journal on Interactive Design and Manufacturing (IJIDeM),* 17(4), 2023: 1933–1947. https://doi.org/10.1007/s12008-023-01312-w

[9] A.K. Dahiya, B.K. Bhuyan, P. Kumar, S. Salunkhe, S. Kumar, Influence of process parameters on kerf properties of GFRP with abrasive water jet machining. *International Journal of Materials Engineering Innovation (IJMATEI),* 14(2), 2023: 123. https://doi.org/10.1504/IJMATEI.2023.130121

[10] M.R.A. Alrasheed, Effective optimization strategies for abrasive water jet machining of glass-carbon fiber reinforced composites: a comparative study of evolutionary optimization techniques. *Journal of Engineering Research*, 13(3), 2024: 1682-1694. https://doi.org/10.1016/j.jer.2024.05.003

[11] K.K. Singh, R.K. Thakur, Experimental analysis on carbon nanotube embedded GFRP composites during AWJM. *Materials and Manufacturing Processes*, 37(2), 2022: 210–220. https://doi.org/10.1080/10426914.2021.1960997

[12] B.G. Vikas, S. Srinivas, Kerf analysis and delamination studies on glass-epoxy composites cut by abrasive water jet. *Materials Today: Proceedings*, 46(Part 10), 2021: 4475–4481. https://doi.org/10.1016/j.matpr.2020.09.683

[13] K.R. Manoj, M. Shet, V. Naveen, S. Murthy, S. Srinivas, Kerf analysis and delamination study on fiber reinforced composites cut by abrasive water jet. *Materials Today: Proceedings*, 46(Part 10), 2021: 5042–5047. https://doi.org/10.1016/j.matpr.2020.10.408

[14] D.K. Jesthi, R.K. Nayak, B.K. Nanda, D. Das, Assessment of abrasive jet machining of carbon and glass fiber reinforced polymer hybrid composites. *Materials Today: Proceedings*, 18(Part 7), 2019: 3116–3121. https://doi.org/10.1016/j.matpr.2019.07.185

[15] D. Deepak, K. Ashwin Pai, Study on abrasive water jet drilling for graphite filled glass/epoxy laminates. *Journal of Mechanical Engineering and Sciences*, 13(2), 2019: 5126–5136. https://doi.org/10.15282/jmes.13.2.2019.24.0421

[16] K.S. Prasad, G. Chaitanya, Selection of optimal process parameters by Taguchi method for drilling GFRP composites using abrasive water jet machining technique. *Materials Today: Proceedings*, 5(9), 2018: 19714–19722. https://doi.org/10.1016/j.matpr.2018.06.333

[17] S. Muralidharan, I. Aatthisugan, A. Tripathi, H. Baradiya, A. Singh, A study on machinability of polymer composite by abrasive water jet machining. *IOP Conference Series: Materials Science and Engineering,* 402, 2018: 012102. https://doi.org/10.1088/1757-899X/402/1/012102

[18] I.W.M. Ming, A.I. Azmi, L.C. Chuan, A.F. Mansor, Experimental study and empirical analyses of abrasive waterjet machining for hybrid carbon/glass fiber-reinforced composites for improved surface quality. *The International Journal of Advanced Manufacturing Technology*, 95(9–12), 2018: 3809–3822. https://doi.org/10.1007/s00170-017-1465-9

[19] P. Thayananthan, N. Yuvaraj, V. Loganathan, Optimizing the machining parameters of abrasive water jet machining for polymer nanocomposite containing tungsten carbide nanoparticles. *Journal of Advanced Engineering Research*, 4(1), 2017: 30-35.

[20] M. Armağan, A.A. Arici, Cutting performance of glass-vinyl ester composite by abrasive water jet. *Materials and Manufacturing Processes*, 32(15), 2017: 1715–1722. https://doi.org/10.1080/10426914.2016.1269919

[21] D. Doreswamy, B. Shivamurthy, D. Anjaiah, N.Y. Sharma, An investigation of abrasive water jet machining on graphite/glass/epoxy composite. *International Journal of Manufacturing Engineering,* 2015(1), 2015: 1–11. https://doi.org/10.1155/2015/627218

[22] E. Lemma, L. Chen, E. Siores, J. Wang, Study of cutting fiber-reinforced composites by using abrasive water-jet with cutting head oscillation. *Composite Structures*, 57(1–4), 2002: 297–303. https://doi.org/10.1016/S0263-8223(02)00097-1

[23] K. Rasu, A. Veerabathiran, Tribological behaviour of industrial waste based agave sisalana/glass fiber reinforced hybrid composites for marine applications. *Materials Testing*, 65(4), 2023: 593–602. https://doi.org/10.1515/mt-2022-0431

[24] R.K. Thakur, K.K. Singh, J. Ramkumar, Impact of nanoclay filler reinforcement on CFRP composite performance during abrasive water jet machining. *Materials and Manufacturing Processes*, 36(11), 2021: 1264–1273. https://doi.org/10.1080/10426914.2021.1906896

[25] F. Bañon, A. Sambruno, P.F. Mayuet, Á. Gómez-Parra, Study of abrasive water jet machining as a texturing operation for thin aluminium alloy UNS A92024. *Materials*, 16(10), 2023: 3843. https://doi.org/10.3390/ma16103843

[26] F. Bañon, A. Sambruno, L. González-Rovira, J. M. Vazquez-Martinez, J. Salguero, A review on the abrasive water-jet machining of metal–carbon fiber hybrid materials. *Metals*, 11(1), 2021: 164. https://doi.org/10.3390/met11010164

[27] M. Hashish, Abrasive waterjet machining. *Materials*, 17(13), 2024: 3273. https://doi.org/10.3390/ma17133273

[28] F. Kartal, Abrasive water jet machining of carbon fiber-reinforced PLA composites: optimization of machinability and surface integrity for high-precision applications. *Polymers*, 17(4), 2025: 445. https://doi.org/10.3390/polym17040445

[29] F. Masoud, S.M. Sapuan, M.K.A.M. Ariffin, Y. Nukman, E. Bayraktar, Experimental analysis of kerf taper angle in cutting process of sugar palm fiber reinforced unsaturated polyester composites with laser beam and abrasive water jet cutting technologies. *Polymers*, 13(15), 2021: 2543. https://doi.org/10.3390/polym13152543

[30] L. Wu, X. Zou, Y. Guo, L. Fu, Experimental research and parameter optimization of high-pressure abrasive water jet machining. *Lubricants*, 13(4), 2025: 153. https://doi.org/10.3390/lubricants13040153

[31] R.K. Thakur, K.K. Singh, Experimental investigation and optimization of abrasive water jet machining parameter on multi-walled carbon nanotube doped epoxy/carbon laminate. *Measurement*, 164, 2020: 108093. https://doi.org/10.1016/j.measurement.2020.108093

[32] A. Abouzaid, S. Mousa, A.M.M. Ibrahim, Effect of standoff distance and traverse speed on the cutting quality during the abrasive water jet machining (AWJM) of brass. *Machining Science and Technology*, 28(3), 2024: 392–414. https://doi.org/10.1080/10910344.2024.2332874

[33] H. Wu, C. Zhou, Z. Pu, X. Lai, H. Yu, D. Li, Experimental investigation on the effects of the standoff distance and the initial radius on the dynamics of a single bubble near a rigid wall in an ultrasonic field. *Ultrasonics Sonochemistry*, 68, 2020: 105197. https://doi.org/10.1016/j.ultsonch.2020.105197